

Experimentally Tractable Generation of High-Order Rogue Waves in Bose-Einstein Condensates

J. Adriaola¹ and P. G. Kevrekidis²

¹*Department of Mathematics, Southern Methodist University, Dallas, TX, USA*

²*Department of Mathematics and Statistics, University of Massachusetts Amherst, Amherst, MA 01003-4515, USA*

(Dated: July 8, 2024)

In this work, we study a prototypical, experimentally accessible scenario that enables the systematic generation of so-called high-order rogue waves in atomic Bose-Einstein condensates. These waveforms lead to *significantly* and *controllably* more extreme focusing events than the famous Peregrine soliton. In one spatial dimension, we showcase conclusive numerical evidence that our scheme generates the focusing behavior associated with the first four rogue waves from the relevant hierarchy. We then extend considerations to anisotropic two-dimensional and even three-dimensional settings, establishing that the scheme can generate second order rogue waves despite the well-known limitation of finite-time blow up of focusing nonlinear Schrödinger equations.

Introduction. Over the last two decades, the study of rogue waves has become one of the most active themes of study within nonlinear science [1–6]. A series of remarkable developments, initially in the field of nonlinear optics [7–13], led to detection tools for probing rogue waves and also suggested their relevance in other applications, such as in supercontinuum generation. Meanwhile, state-of-the-art experiments in fluid mechanics [14–16] not only enabled the realization of the famous prototypical Peregrine soliton nonlinear waveform [17], but also a higher-order breather referred to as a “super rogue wave” [15]. Importantly, other areas of dispersive wave dynamics including plasmas [18–20] and more recently atomic Bose-Einstein condensates [21] have offered additional fertile platforms for the exploration of associated rogue wave dynamics.

What is perhaps less familiar in the physics community is how these rogue waves naturally emerge in different wave-breaking scenarios of dispersive wave PDE models. Here, we argue that such an understanding proves essential to their physical implementation and immediately provides an experimentally tractable example. Starting with the universal Korteweg-de Vries equation, a famous Dubrovin conjecture proved in [22] characterized wave breaking as described by a solution of the second member of the Painlevé-I hierarchy. Similarly, for the universal nonlinear Schrödinger (NLS) model, the proof of another Dubrovin conjecture in [23] established the wave-breaking description via a solution of the tritonquée solution of the Painlevé-I equation. The work of [24] obtained similar results for the Sine-Gordon model.

Our focus herein involves a less generic, yet still very much experimentally tractable scenario involving the NLS equation; a ubiquitous physics model that arises in nonlinear optics [25, 26], atomic physics [27–29] and plasma dynamics [30]. The NLS equation features a non-generic focusing example based on a Painlevé-III type breaking known to arise from the so-called Talanov, or semi-circle, initial data [31, 32]. As recently explained in [33], the dispersionless limit of this problem exhibits a finite-time blow up with the presence of dispersion manifesting so-called high-order rogue waves

(HORWs). Reference [34] shows how HORWs can be obtained via Darboux transformations while references [35, 36] provide a more mathematically detailed study thereof. Indeed, this process has an asymptotic limit, namely the so-called infinite-order rogue wave that was identified, for the first time to our knowledge, in the work of [37].

Our aim is to show that atomic Bose-Einstein condensates present an excellent opportunity for the generation of high-order, and potentially infinite order, rogue waves dynamically. This is due to the fact that in the well-known Thomas-Fermi (TF) limit of large density, such systems under self-defocusing (self-repulsive) nonlinearity acquire a well-established parabolic density profile [27–29], up to a small boundary-layer and curvature-driven correction that has been analyzed in [38, 39].

This provides approximately semi-circular initial wavefunction data “for free”, as it is the ground state of the self-repulsive problem provided that one can perform a quench in the nonlinearity from the defocusing to the focusing, modulationally unstable regime. Fortunately, such quenches are known to be quite feasible in atomic BECs, from the early works of [40, 41], demonstrations of wide tunability in [42], and even the recent realization of Townes soliton collapse in [43]. Indeed, the very recent work of [44] has used such a quench to probe the collapse of a vortical BEC pattern.

We show that this technique can be tuned through the chemical potential, the trap strength, and the scattering length to provide good approximations of k^{th} -order rogue waves for $k = 2$, $k = 3$ and $k = 4$, with the potential to, in principle, generalize this approach to higher orders. We then go beyond one-dimensional settings, as is more realistic in atomic BECs, and illustrate that even higher-dimensional settings with a quasi-1D confinement *still* provide the possibility of an excitation of higher order rogue waves such as $k = 2$ and $k = 3$. This, in turn, strongly suggests that many of the above experiments bear the controllable formation of such higher-order rogue waves at their fingertips and the experimental range to which this technology can be used to obtain excitations of large am-

plitude waveforms still remains to be (hopefully, imminently) explored.

Theoretical Analysis of HORWs. To briefly provide the theoretical background of the type of rogue waves that we consider throughout this work, we closely follow the concise account of Bilman, et al. [35]. We begin by considering the prototypical focusing NLS equation

$$i\partial_t\psi = -\frac{1}{2}\partial_x^2\psi - |\psi|^2\psi, \quad (1)$$

where $x \in \mathbb{R}$. A potential term $V(x)\psi$ added to the right hand side of (1) will also (when appropriate) be considered in the numerical examples that follow. Notice that for all considerations below, for breadth of exposition, we will maintain our quantities dimensionless. Numerous systematic topical expositions, e.g., in atomic physics [27–29] or optics [25, 26] detail how to translate these general findings to dimensional units, as needed.

An expression of the HORWs that exactly solve the NLS equation (1) can be constructed through the following procedure. Consider the expansion coefficients from the suitable series expansion around $\lambda = i$, $F_\ell(x, t)$ and $G_\ell(x, t)$, where $\ell \in \mathbb{Z}^+$, arising from the generating functions

$$(1 - i\lambda) \frac{\sin\left((x + \lambda t)\sqrt{\lambda^2 + 1}\right)}{\sqrt{\lambda^2 + 1}} = \sum_{\ell=0}^{\infty} \left(\frac{i}{2}\right)^\ell F_\ell(x, t)(\lambda - i)^\ell,$$

$$\cos\left((x + \lambda t)\sqrt{\lambda^2 + 1}\right) = \sum_{\ell=0}^{\infty} \left(\frac{i}{2}\right)^\ell G_\ell(x, t)(\lambda - i)^\ell.$$

We use these coefficients to define the following $k \times k$ matrices

$$K_{pq}^{(k)}(x, t) := \sum_{\mu=0}^{p-1} \sum_{\nu=0}^{q-1} \binom{\mu + \nu}{\mu} \left(F_{q-\nu-1}^* F_{p-\mu-1} + G_{q-\nu-1}^* G_{p-\mu-1} \right),$$

and

$$H_{pq}^{(k)}(x, t) := -2(F_{p-1} + G_{p-1}) \left(F_{q-1}^* - G_{q-1}^* \right),$$

where $1 \leq p, q \leq k$ and with $*$ denoting complex conjugation, while the arguments of F and G , being (x, t) , are implied for brevity.

Rogue waves of order k , denoted by $\psi_k(x, t)$, are thus furnished by the following formula

$$\psi_k(x, t) := (-1)^k \frac{\det(\mathbf{K}^{(k)}(x, t) + \mathbf{H}^{(k)}(x, t))}{\det(\mathbf{K}^{(k)}(x, t))}. \quad (2)$$

For example, the $k = 1$ Peregrine solution, up to an unimportant phase factor, is given by

$$\psi_1(x, t) := 1 - 4 \frac{1 + 2it}{1 + 4x^2 + 4t^2}.$$

The compact representation afforded by Equation (2) coincides

with the leading order solution of a parametrized matrix Riemann-Hilbert problem. See [35], in particular Proposition 1, for more details.

We show the space-time evolution of the first four of these rogue waves, in absolute value, in Figure 1. Note that this process can be generalized for arbitrary k , leading eventually to the limit of $k \rightarrow \infty$ which corresponds to the waveform discovered in [37]. The sequence of the states, through having k “stems” and from which an extreme focusing emerges, is transparent in the space-time evolution of the patterns in Figure 1.

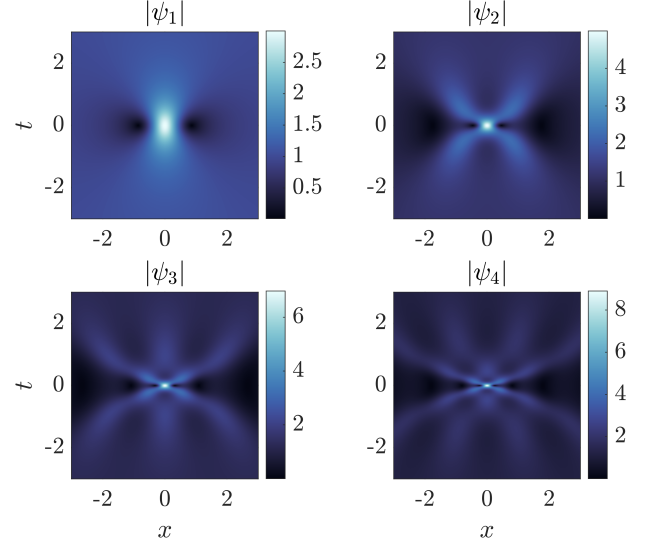


Figure 1. Visualization of the first four NLS rogue waves, in absolute value, whose formulae are given by Equation (2) and the immediately preceding definitions.

Numerical Examples: the One-Dimensional Case. We now turn to the one-dimensional realization of our proposed experimental protocol (within atomic BECs [27–29], or, by extension, optical media with parabolic refractive index; see, e.g., [45, 46] for some relevant examples). We start at the defocusing regime with a parabolic confinement $V(x) = (1/2)\Omega^2 x^2$ and nonlinear defocusing prefactor g_{defocus} , for a controllable chemical potential μ ; both μ and Ω are tunable, and $\mu \gg \Omega$ defines the effective TF regime. The ground state wavefunction is approximately semicircular with density controllably approximated by $|\psi_{TF}|^2 = \mu - V(x)$, where $\mu > V(x)$. The approximation becomes progressively better as the TF regime is approached, with an accordingly shrinking boundary layer (see, also [38, 39]).

Now, at $t = 0$, we switch the nonlinearity to a focusing one of prefactor g_{focus} , i.e., solving Eq. (1), but with (again, controllable attractive interactions [41, 42, 47]) nonlinear prefactor g_{focus} and with this controllably close to a semi-circular initial condition. We use imaginary-time propagation [48] to compute the ground state with evolution, here and in the focusing case, computed via an adaptize step-size split-step

method [49].

To make the claim that this protocol enables the controlled generation (as the parameters μ , g and Ω are varied) of high-order rogue waves, we perform a fit of our numerical realizations thereof, at the time of maximal focusing, to the exact solutions given by Equation (2) rescaled appropriately in space and by the value of the nonlinear focusing coefficient g_{focus} such that the NLS equation (1) remains invariant.

We denote the rescaling in space used to minimize the mismatch in the $L^2(\mathbb{R})$ norm between the numerics and the exact solution by the symbol s . Since the functions given by Equation (2) have a non-zero background, we minimize the mismatch centered at space and up until the absolute value reaches its last local minimum to the left and to the right of the origin. In the figure captions, we report the parameters $(\Omega, g_{\text{defocus}}, g_{\text{focus}}, \mu, s)$ found via optimization that minimize the mismatch between numerical simulations and the exact formula given by Equation (2). We use the differential evolution method [50] in the optimization.

In Figure 2, we show the match between the first four generated rogue waves and the exact expressions from Equation (2). Naturally, and similarly to what occurs in the case of the single Peregrine in BECs [21], we can only hope to *locally* match the k -th order rogue waves, given the distinct nature of the spatial asymptotics of our initial conditions, hence the need for our proposed matching selection. Nevertheless, our fitting procedure clearly suggests the local spontaneous generation of the relevant multi-hump patterns, by analogy with what happens for Peregrine-based wave breaking in [23].

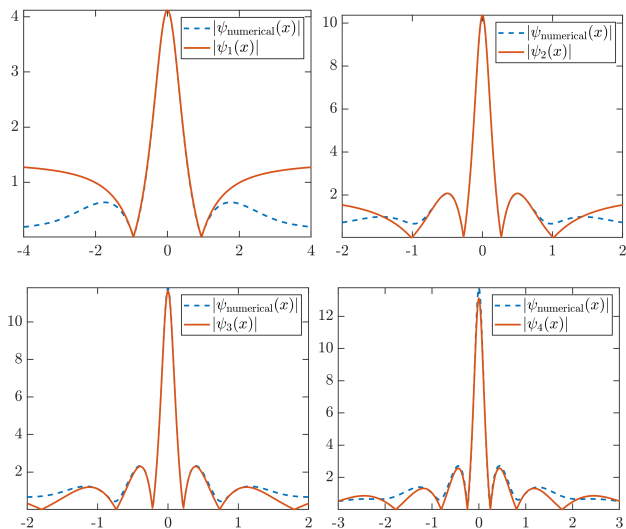


Figure 2. Local fitting of our numerical simulations to the first 4 (i.e., $k = 1$ to $k = 4$) HORWs given by Equation (2). We report the parameters $(\Omega, g_{\text{defocus}}, g_{\text{focus}}, \mu, s)$ to three digits of precision. Top left: (1.06, 0.87, -0.443, 3.42, 0.914). Top right: (1.23, 0.891, -0.701, 6.19, 1.74). Bottom Left: (1.25, 1.07, -0.794, 7.42, 1.49). Bottom Right: (1.93, 1.84, -0.483, 18.2, 1.01).

Higher-dimensional Generalizations. Extending considerations to two spatial dimensions, we are able to observe HORWs, e.g., with $k = 2$ or $k = 3$ in anisotropic variants of the latter setting. More concretely, we show the formation of focusing strongly reminiscent of a second order rogue wave in the top panel of Figure 3. It is clear here that we need an experimentally accessible, highly anisotropic 2D trap $V(x, y) = \frac{\Omega_x^2}{2}x^2 + \frac{\Omega_y^2}{2}y^2$ in order to achieve the relevant dynamics. We further show the shape of the initial condition used to illustrate the level of anisotropy used to ensure the prevention of finite-time blowup of the dynamics. During the focusing dynamics, we release the trap in the x -direction while maintaining the trap in the transverse, that is, y -direction fixed. In the bottom panel of Figure 3, we show the formation of a $k = 3$ rogue wave, as well as an isosurface of the two-dimensional dynamics.

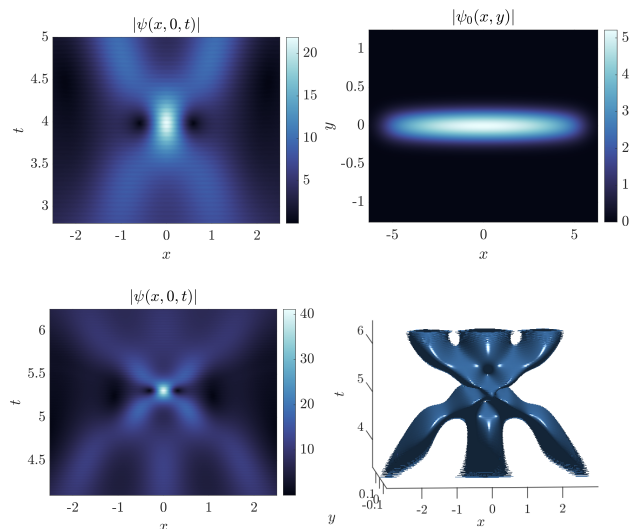


Figure 3. Top panels: A two-dimensional simulation showing second order rogue wave-type behavior and the highly anisotropic nature of the initial condition. The parameters used here are $\Omega_x = 1$, $\Omega_y = 60$, $\mu = 42.7$, $g_{\text{defocus}} = 1$, and $g_{\text{focus}} = -0.05$. Bottom panels: third order rogue wave-type behavior. The parameters used here are $\Omega_x = .75$, $\Omega_y = 100$, $\mu = 71.1$, $g_{\text{defocus}} = 1$, and $g_{\text{focus}} = -0.05$. An isosurface of constant value 55 displays the profile, in absolute-value squared, of the dynamics.

In three spatial dimensions, anisotropy can once again serve to mitigate the risk of collapse, as is well-known, e.g., from works such as [51–53]. This, in turn, enables us, within the regimes of sufficiently tightly transversely confined BECs discussed therein, to identify parameters that lead to a genuine second order rogue wave-type scenario. This is shown in Fig. 4 both at the level of the quasi-1D space-time evolution (left panel) and at that of the detailed comparison of the main feature in a quasi-1D integrated form with the 2nd order rogue wave of the Equation (2).

Conclusions and Future Challenges. In the present work we revisited the framework of higher-order rogue waves that

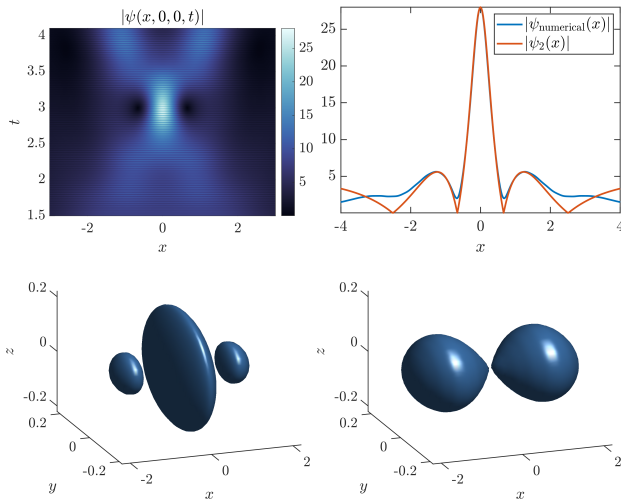


Figure 4. A three-dimensional simulation that yields a second order rogue wave-type behavior performed from a defocusing ground state prepared with $\Omega_x = 1$, $\Omega_y = \Omega_z = 100$, $\mu = 143$, and a defocusing coefficient of $g_{\text{defocus}} = 1$. The top left panel shows the space-time evolution for $g_{\text{focus}} = -.05$ in the elongated direction x . The top right panel shows a corresponding comparison of the central feature with the 2nd order rogue wave of Equation (2). The bottom panels are three-dimensional isosurfaces revealing the focusing structure at time 3 in absolute-value 12 (left) and time 4.2 in absolute-value 20 (right).

has been recently developed in the mathematical literature (via Darboux transformations and robust inverse scattering methods) as a *non-generic, yet well-accessible* form of wave breaking. While, to the best of our knowledge, this setup has not

been explored at the level of realistic or experimentally relevant settings, we have showcased examples that are *fully accessible* to current atomic BEC experiments (and also elsewhere, such as, e.g., suitably designed optical media). We then went on to explore the freedom available to the system through a variation of parameters to provide scenarios enabling the realization of $k = 1$ through $k = 4$ rogue waves, with a view towards higher order rogue waves, including the intriguing infinite-order one of [37]. While the relevant idea is, in its essence, tailored to one spatial dimension, we have illustrated that higher-dimensional, highly anisotropic settings are also very much accessible and conducive towards such considerations.

Naturally, this study paves the way for numerous further considerations of related concepts. We only mention a few of these here. One necessity is a wide parametric mapping of the space of possible outcomes of near-semi-circular initial data in the space of (μ, Ω) etc. Another question: how amenable are non-integrable systems to such types of wave breaking? For example, will HORW-type behavior survive in quintic, cubic-quintic, or other recently proposed so-called droplet [54] variants of the model? A further direction stems from spatially discrete models and concerns whether a variant of such higher-order (including infinite-order [37]) rogue waves exists of Ablowitz-Ladik type and discrete nonlinear Schrödinger type lattices [55, 56].

It can thus be inferred that this theme presents a wide palette of opportunities in one- and higher- spatial dimensions that are extremely timely and relevant for near-future analytical, numerical and experimental considerations.

-
- [1] Z. Yan, *J. Phys.: Conf. Ser.* **400**, 012084 (2012).
- [2] M. Onorato, S. Residori, U. Bortolozzo, A. Montina, and F. T. Arecchi, *Phys. Rep.* **528**, 47 (2013).
- [3] J. M. Dudley, F. Dias, M. Erkintalo, and G. Genty, *Nature Photon* **8**, 755 (2014).
- [4] D. Mihalache, *Rom. Rep. Phys.* **69**, 403 (2017).
- [5] J. M. Dudley, G. Genty, A. Mussot, A. Chabchoub, and F. Dias, *Nat Rev Phys* **1**, 675 (2019).
- [6] A. Tikan, S. Randoux, G. El, A. Tovbis, F. Copie, and P. Suret, *Front. Phys.* **8** (2021).
- [7] D. R. Solli, C. Ropers, P. Koonath, and B. Jalali, *Nature* **450**, 1054 (2007).
- [8] D. R. Solli, C. Ropers, and B. Jalali, *Phys. Rev. Lett.* **101**, 233902 (2008).
- [9] B. Kibler, J. Fatome, C. Finot, G. Millot, F. Dias, G. Genty, N. Akhmediev, and J. M. Dudley, *Nature Phys* **6**, 790 (2010).
- [10] B. Kibler, J. Fatome, C. Finot, G. Millot, G. Genty, B. Wetzell, N. Akhmediev, F. Dias, and J. M. Dudley, *Sci. Rep.* **2**, 463 (2012).
- [11] P. T. S. DeVore, D. R. Solli, D. Borlaug, C. Ropers, and B. Jalali, *J. Opt.* **15**, 064001 (2013).
- [12] B. Frisquet, B. Kibler, P. Morin, F. Baronio, M. Conforti, G. Millot, and S. Wabnitz, *Sci Rep* **6**, 20785 (2016).
- [13] A. Tikan, C. Billet, G. El, A. Tovbis, M. Bertola, T. Sylvestre, F. Gustave, S. Randoux, G. Genty, P. Suret, and J. M. Dudley, *Phys. Rev. Lett.* **119**, 033901 (2017).
- [14] A. Chabchoub, N. P. Hoffmann, and N. Akhmediev, *Phys. Rev. Lett.* **106**, 204502 (2011).
- [15] A. Chabchoub, N. Hoffmann, M. Onorato, and N. Akhmediev, *Phys. Rev. X* **2**, 011015 (2012).
- [16] A. Chabchoub and M. Fink, *Phys. Rev. Lett.* **112**, 124101 (2014).
- [17] D. H. Peregrine, *J. Aust. Math. Soc. Series B, Appl. Math.* **25**, 16 (1983).
- [18] H. Bailung, S. K. Sharma, and Y. Nakamura, *Phys. Rev. Lett.* **107**, 255005 (2011).
- [19] R. Sabry, W. M. Moslem, and P. K. Shukla, *Phys. Plasmas* **19**, 122903 (2012).
- [20] R. E. Tolba, W. M. Moslem, N. A. El-Bedwehy, and S. K. El-Labany, *Phys. Plasmas* **22**, 043707 (2015).
- [21] A. Romero-Ros, G. C. Katsimiga, S. I. Mistakidis, S. Mossman, G. Biondini, P. Schmelcher, P. Engels, and P. G. Kevrekidis, *Phys. Rev. Lett.* **132**, 033402 (2024).
- [22] T. Claeys and T. Grava, *Communications in Mathematical*

- Physics **286**, 979 (2009).
- [23] M. Bertola and A. Tovbis, *Commun. Pure Appl. Math.* **66**, 678 (2013).
- [24] B.-Y. Lu and P. Miller, *Communications on Pure and Applied Mathematics* **75**, 1517 (2022), <https://onlinelibrary.wiley.com/doi/pdf/10.1002/cpa.22018>.
- [25] Y. S. Kivshar and G. P. Agrawal, *Optical Solitons: From Fibers to Photonic Crystals* (Academic Press, 2003) pp. 1–540.
- [26] A. Hasegawa and Y. Kodama, *Solitons in Optical Communications* (Clarendon Press, Oxford, 1995).
- [27] L. Pitaevskii and S. Stringari, *Bose-Einstein condensation* (Oxford University Press, Oxford, 2003).
- [28] C. J. Pethick and H. Smith, *Bose-Einstein Condensation in Dilute Gases* (Cambridge University Press, Cambridge, United Kingdom, 2002).
- [29] P. G. Kevrekidis, D. J. Frantzeskakis, and R. Carretero-González, *The Defocusing Nonlinear Schrödinger Equation* (SIAM, Philadelphia, 2015).
- [30] M. Kono and M. Skorić, *Nonlinear Physics of Plasmas* (Springer-Verlag, Heidelberg, 2010).
- [31] V. Talanov, *Journal of Experimental and Theoretical Physics* (1970).
- [32] A. Gurevich and A. Shvartsburg, *Journal of Experimental and Theoretical Physics* (1970).
- [33] F. Demontis, G. Ortenzi, G. Roberti, and M. Sommacal, *Phys. Rev. E* **108**, 024213 (2023).
- [34] J. S. He, H. R. Zhang, L. H. Wang, K. Porsezian, and A. S. Fokas, *Phys. Rev. E* **87**, 052914 (2013).
- [35] D. Bilman, L. Ling, and P. D. Miller, *Duke Mathematical Journal* **169** (2020), 10.1215/00127094-2019-0066.
- [36] D. Bilman and P. D. Miller, *Physica D: Nonlinear Phenomena* **435**, 133289 (2022).
- [37] B. Suleimanov, *JETP Letters* **106**, 400 (2017).
- [38] G. Karali and C. Sourdis, *Archive for Rational Mechanics and Analysis* **217**, 439 (2015).
- [39] C. Gallo and D. E. Pelinovsky, *Asymptot. Anal.* **73**, 53 (2009).
- [40] S. L. Cornish, N. R. Claussen, J. L. Roberts, E. A. Cornell, and C. E. Wieman, *Phys. Rev. Lett.* **85**, 1795 (2000).
- [41] J. L. Roberts, N. R. Claussen, S. L. Cornish, E. A. Donley, E. A. Cornell, and C. E. Wieman, *Phys. Rev. Lett.* **86**, 4211 (2001).
- [42] S. E. Pollack, D. Dries, M. Junker, Y. P. Chen, T. A. Corcovilos, and R. G. Hulet, *Phys. Rev. Lett.* **102**, 090402 (2009).
- [43] C.-A. Chen and C.-L. Hung, *Phys. Rev. Lett.* **125**, 250401 (2020).
- [44] S. Banerjee, K. Zhou, S. K. Tiwari, H. Tamura, R. Li, P. Kevrekidis, S. I. Mistakidis, V. Walther, and C.-L. Hung, “Collapse of a quantum vortex in an attractive two-dimensional bose gas,” (2024), [arXiv:2406.00863](https://arxiv.org/abs/2406.00863) [cond-mat.quant-gas].
- [45] S. Longhi, *Opt. Lett.* **28**, 2363 (2003).
- [46] M. Conforti, C. M. Arabi, A. Mussot, and A. Kudlinski, *Opt. Lett.* **42**, 4004 (2017).
- [47] E. A. Donley, N. R. Claussen, S. L. Cornish, J. L. Roberts, E. A. Cornell, and C. E. Wieman, *Nature* **412**, 295–299 (2001).
- [48] W. Bao and Q. Du, “Computing the ground state solution of bose-einstein condensates by a normalized gradient flow,” (2003), [arXiv:cond-mat/0303241](https://arxiv.org/abs/cond-mat/0303241) [cond-mat].
- [49] O. V. Sinkin, R. Holzlohner, J. Zweck, and C. R. Menyuk, *Journal of lightwave technology* **21**, 61 (2003).
- [50] R. Storn and K. Price, *J. Global Optim.* **11**, 341 (1997).
- [51] V. M. Pérez-García, H. Michinel, J. I. Cirac, M. Lewenstein, and P. Zoller, *Phys. Rev. A* **56**, 1424 (1997).
- [52] L. Salasnich, A. Parola, and L. Reatto, *Phys. Rev. A* **66**, 043603 (2002).
- [53] C. Márquez and E. Evaristo, Master’s Thesis (2014).
- [54] Z.-H. Luo, W. Pang, B. Liu, Y.-Y. Li, and B. A. Malomed, *Front. Phys.* **16**, 1 (2021).
- [55] M. Ablowitz, B. Prinari, and A. Trubatch, *Discrete and Continuous Nonlinear Schrödinger Systems* (Cambridge University Press, Cambridge, 2004).
- [56] P. G. Kevrekidis, *The Discrete Nonlinear Schrödinger Equation* (Springer Berlin Heidelberg, 2009).